WARSAW UNIVERSITY OF TECHNOLOGY Index 351733
FACULTY OF CIVIL ENGINEERING
COMMITTEE FOR CIVIL AND WATER ENGINEERING
POLISH ACADEMY OF SCIENCES ISSN 1230-2945
DOI: 10.24425/ace.2024.150971
ARCHIVES OF CIVIL ENGINEERING
Vol. LXX ISSUE 3 2024
pp. 71–84
© 2024. Marcin Kozłowski, Dominik Wasik, Maciej Cwyl.

This is an open-access article distributed under the terms of the Creative Commons Attribution-NonCommercial-NoDerivatives License (CC BY-NC-ND 4.0, https://creativecommons.org/licenses/by-nc-nd/4.0/), which permits use, distribution, and reproduction in any medium, provided that the Article is properly cited, the use is non-commercial, and no modifications or adaptations are made.

**Research paper**

# Experimental studies on metal-glass point connections with various configurations of mesh reinforcement

**Marcin Kozłowski[1], Dominik Wasik[2], Maciej Cwyl[3]**

**Abstract:** The paper deals with the phenomenon of post-breakage capacity in point-fixed laminated glass elements. It reports the results of an ongoing research project aimed at developing a reinforced point-fixed laminated glass element with locally embedded steel mesh. In total, 36 specimens ($300 \times 300$ mm$^2$) varying in the thickness of component panes (8, 10 and 12 mm) and the diameter of the reinforcing inserts (75, 110 and 150 mm) were tested. The specimens comprised two toughened glass panes, an EVA Clear interlayer and a woven steel mesh consisting of wires (0.35 mm in diameter) at a spacing of $1 \times 1$ mm$^2$. The tests were carried out in a spatial testing machine allowing the point connector to be loaded at an angle of 45 degrees. This way of loading the fastener corresponds to its loading condition in an actual application (e.g. a glass canopy with diagonal rods). All samples presented similar behaviour during testing. In the first phase, the relationship between the load and the displacement refers to the elastic response of the sample to the load. Following the glass failure, there is a sudden drop in the force due to the loss of tensile stiffness of fractured glass. After this stage, progressive degradation of the samples occurs due to further loading. In this phase, the force is initially increasing and stabilising – this point is considered an ultimate failure (in the post-breakage phase), and the experiment is terminated. For all test series, the reinforcement increases the post-breakage capacity.

**Keywords:** laminated glass, point connections, reinforcement, post-breakage capacity

[1]DSc., PhD., Eng., Silesian University of Technology, Faculty of Civil Engineering, Akademicka 5, 44-100 Gliwice, Poland, e-mail: marcin.kozlowski@polsl.pl, ORCID: 0000-0002-1698-023X
[2]MSc., Silesian University of Technology, Faculty of Civil Engineering, Akademicka 5, 44-100 Gliwice, Poland, e-mail: dominik.wasik@polsl.pl, ORCID: 0000-0001-8654-4479
[3]PhD., Eng., Warsaw University of Technology, Faculty of Civil Engineering, Al. Armii Ludowej 16, 00-637 Warsaw, Poland, e-mail: maciej.cwyl@pw.edu.pl, ORCID: 0000-0002-2894-7840

# 1. Introduction

Glass has been a fascinating material to humankind since Egyptians first made it [1]. Glass is one of the most versatile and oldest materials used in the construction industry. Initially, glass was used to fill window frames; nowadays, it is used to make structural elements of buildings [2]. The reason for using glass nowadays as a structural element is the desire to bring much natural sunlight into the buildings [3]. Glass is used as a material for making elements that can carry live loads. Examples of such elements are glass facades, stairs and balustrades, and recently very popular canopies over building entrances. The use of float glass in such elements would be impossible for safety reasons [4]. Monolithic glass is a brittle material, it does not have the ability to plastic deformation or energy absorption at the moment of impact [5]. In structural elements made of glass, it is necessary to use the so-called laminated glass (safety glass). Laminated glass is a permanent connection of two or more fully tempered glass panes with a special laminating film (interlayer) [6].

The behaviour of safety glass after failure is significantly different from float glass. Fully tempered glass, when fractured, breaks into small pieces, which are then held together by an interlayer [7]. Due to such behaviour, the damaged structure can maintain sufficient structural integrity and load-bearing capacity to enable efficient evacuation of people and avoid injuries, as well as safely replace damaged elements [8].

Determining the behaviour of glass in the elastic phase and the moment of its cracking using FEM models is possible to reproduce with satisfactory accuracy, as in publications [9–11]. Nevertheless, the post-breakage behaviour of laminated glass is still an unknown problem. This is because due to the behaviour of the glass and the lack of unified material parameters, the analytical and numerical models in this phase are unclear. Destructive laboratory tests are the simplest way to determine the strength of the glass in the post-breakage phase. At today's level of knowledge, it is possible to determine the approximate post-breakage phase capacity of glass using FEM models. However, this issue requires experimental research and appropriate numerical model validation each time.

The problem of post-breakage load capacity is an issue reluctantly undertaken by scientists. In research [12], it was found that the results for testing samples in the post-breakage phase depend strictly on the arrangement of glass cracks. In subsequent tests [13], it was found that the tension stiffening effect, together with the pre-compression of fractured glass pieces, can determine to the partial post-breakage capacity to tensile load. In the tests in [14], point-fixed glass laminates with different interlayers were subjected to drop tests. After scratching, the samples were subjected to a permanent load applied at the centre of the sample span at different temperatures. The fractured elements were able to carry a limited load for some time. In theory, this time would allow people to evacuate from the building safely. Carrying out post-breakage capacity tests is a time-consuming and expensive issue. The high testing costs are caused by the prices of glass laminates (glass and interlayer), the design of an appropriate test stand and the costs of laboratory equipment.

Numerical analysis of laminated glass in the cracked phase requires a non-standard approach to the problem. In article [15], the reaction of a glass laminate to a hard body impact was recreated using combined FEM and DEM. In the simulations, a crack pattern comparable to the

results of experimental tests was obtained. In laboratory tests, the glass laminates' post-breakage capacity was increased with additional materials. In publications [16, 17], laminated glass beams were reinforced by laminating rods made of different materials. During the tests, it was found that additional rods after the glass fracture effectively transferred part of the tensile stresses increasing the strength after cracking glass.

The last example of reinforcement glass laminates was researched by Achintha [18, 19]. In the tests, glass laminates reinforced by laminating inserts made of GFRP near the openings were subjected to in-plane loading. Laminated inserts did not have a beneficial effect on increasing the fracturing force of the glass, but contributed to an increase in strength after breakage by 250% as opposed to the reference samples.

An ongoing project funded by the National Center for Research and Development (NCBR) within the LIDER XI program investigates the idea of laminating a steel woven mesh to glass laminates [20]. The reinforcing steel mesh is designed to improve the load-bearing capacity of the specimen in the post-breakage stage, thus improving the safety of people in the building and ensuring adequate time for evacuation.

This research deals with the post-breakage capacity of laminated glass elements subjected to out-plane loading at an angle of 45° and reports the results of an experimental campaign on the pull-through resistance of laminated glass with embedded steel woven mesh. The most popular structural elements subjected to out-plane loading at an angle of 45° are glass canopies over the entrance to the building, shown in Fig. 1.

Fig. 1. Glass canopy over building entrance

# 2. Materials and methods

## 2.1. Materials

In the study, an ordinary, commercial soda–lime–silicate glass was utilised. Float glass panes were made of fully tempered (toughened) glass due to stress concentrations that typically develop near the holes in loaded samples. Due to the heat-treating process, the toughened glass

shows a characteristic flexural strength of 120 MPa [21]. It is approximately 2–3 times higher than that of annealed float glass [21]. To laminate the panes, an ethylene vinyl acetate (EVA) interlayer was used [4]. All steel elements of the test setup were made of S355-grade steel [22]. Steel woven mesh was made of stainless steel grade 1.4301. Threaded rods were made of 8.8 class bolts. Polytetrafluoroethylene (PTFE) spacers were applied between the steel components and glass to avoid stress concentrations that could lead to premature failure of glass.

## 2.2. Test specimens

Laminated glass samples with dimensions of $300 \times 300$ mm$^2$ were used in the study. The samples comprised two glass panes and two EVA Clear interlayers with a total thickness of 3.04 mm, see Fig. 2. While the thickness of the interlayer was constant for all samples, the thickness of the glass panes varied (8, 10 and 12 mm). In all panes, the waterjet technique produced a central hole with a diameter of 20 mm for point fixing. In the study, two types of samples were produced. In the case of reinforced specimens (RS), a circular woven stainless-steel mesh of different diameters was placed centrally between two layers of the interlayer before the lamination process. After applying temperature in an autoclave, the mesh melted into the foil, making a composite layer. The mesh was composed of 0.35 mm wires at a spacing of $1 \times 1$ mm$^2$. Within RS samples, three different diameters of the reinforcement were applied (75, 110 and 150 mm). Unreinforced samples (REF) were produced as reference samples.

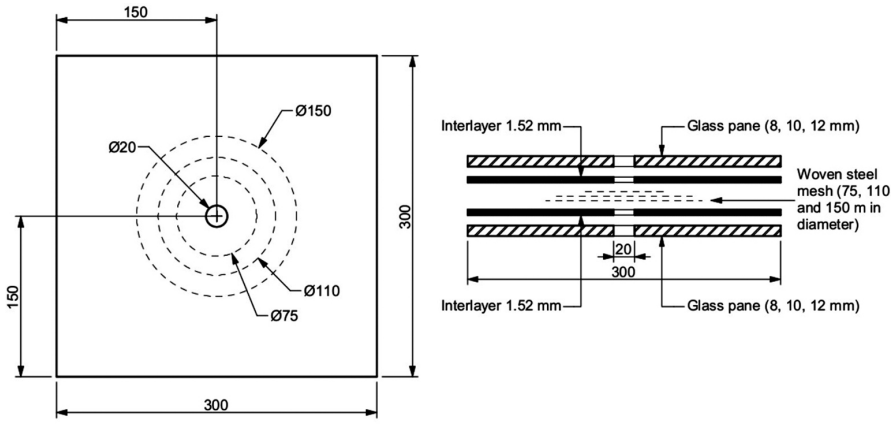


Fig. 2. Exploded cross-section of produced samples

Assuming four repetitions for a single test series, in total, 12 test series (48 specimens) were produced, see Table 1. In the test series, "G" stands for glass build-up, while "R" indicates the diameter of the steel mesh in the reinforced samples.

Table 1. Overview of produced specimens

| Test series | Samples | Glass thickness | Interlayer | Reinforcement |
|---|---|---|---|---|
| G8 | G8-REF<br>G8-R75<br>G8-R110<br>G8-R150 | 2 × 8 mm | 2 × 1.52 mm<br>(EVA Clear) | –<br>Ø75 mm<br>Ø110 mm<br>Ø150 mm |
| G10 | G10-REF<br>G10-R75<br>G10-R110<br>G10-R150 | 2 × 8 mm | 2 × 1.52 mm<br>(EVA Clear) | –<br>Ø75 mm<br>Ø110 mm<br>Ø150 mm |
| G12 | G12-REF<br>G12-R75<br>G12-R110<br>G12-R150 | 2 × 8 mm | 2 × 1.52 mm<br>(EVA Clear) | –<br>Ø75 mm<br>Ø110 mm<br>Ø150 mm |

## 2.3. Testing procedure

The laboratory tests of the analysed joints utilised a specialised multi-directional strength machine, as shown in Fig. 3. It was specifically designed for conducting multidirectional strength tests on connections and structural elements with eight independent actuators, capable of producing a force of up to approximately 350 kN each, at any predetermined angle. Additionally, displacements can be controlled simultaneously, with each actuator able to cause up to 360 mm displacement. During the test process, cameras coupled with software can record laboratory parameters. The results of displacements and forces on individual actuators can be obtained using the recorded test video. The laboratory test can also be linked with additional sensors, such as strain and inductive sensors, which can be correlated with the recorded image. The machine can carry out static and up to 15 Hz dynamic tests, with each actuator able to vibrate at a different frequency. Furthermore, the test stand can be utilised for long-term tests with alternate long-term loading of elements, typically used to analyse fatigue phenomena of materials.

Fig. 3. Test stand for multi-directional strength testing

A static test was conducted to represent the loading conditions of the connections in the glass panels mounted on a building's wall. The load was applied in two planes: one parallel to the glass façade (representing the weight of the cladding) and one perpendicular to it (representing wind action). The resultant force was angled to the façade plane. For testing the connections, actuators applied a force in the plane of the curtain wall. The load was incrementally increased until the samples failed, and the post-critical load capacity of the tested connections was fully described. The mounting station used for the tested elements consisted of a $510 \times 510 \times 20$ mm$^3$ horizontal steel sheet with steel brackets attached to it. A plastic washer measuring $300 \times 300 \times 5$ mm$^3$ with a hole 155 mm in diameter in the middle was permanently attached to the sheet, see Fig. 4. To facilitate the assembly and disassembly of the glass packages, angle bars were welded to the bottom of the sheet, which was then stiffened with $50 \times 50 \times 5$ brackets. The entire substructure was fastened to the testing machine's guides with M12 class 8.8 screws.

Fig. 4. Elements of the test stand mounted in a testing machine

A sample was inserted into the spatial test stand, and a socket was installed (Fig. 5). The socket included an M12 screw (class 5.6), two steel discs with a diameter of 50 mm and thickness of 10 mm, two plastic discs with a diameter of 50 mm and thickness of 4 mm, a steel tube with a height of 10 mm and diameter of 15 mm wrapped with insulating tape, and an eye nut.

Fig. 5. Elements of the test stand mounted in a testing machine

A 10 mm ($6 \times 37$ mm$^2$) steel cable was coiled twice and secured with a steel screw to connect the socket to the testing machine's cylinder. The actuator was positioned at a 45-degree angle to the horizontal sheet, with its axis aligned with the centre of the sample being tested. The socket was placed in the glazing unit, ensuring the eye nut's axis matched the actuator's longitudinal axis. Prior to the strength test, the fastening cable was pre-tensioned. The socket of each sample was pulled at a rate of 10 mm per minute, and the study continued until the post-critical force stabilised. The time, piston displacement and transmitted force were recorded during the tests. The test was recorded using a camera attached to a testing machine.

# 3. Results and discussion

## 3.1. Load-deflection behaviour

Exemplary results of G10 series, including reference and reinforced samples, are displayed in Fig. 6. During the tests, the samples showed multi-stage mechanism of failure, and the behaviour can be divided into three phases. In the elastic phase, the load-displacement relationship is almost linear, indicating the elastic response of the samples to the load. The initial lower angle of the relationship is related to the arrangement of the samples in the test setup. In this stage, the stresses in the glass increase until the limit value is reached, causing the glass to fracture brittlely. In this phase, the force drops significantly as the fractured glass loses its ability to resist tension. In the post-fracture state, the samples gradually deteriorate as they are subjected to additional loading. The force initially increases and then stabilises, with the point of ultimate failure being reached and the experiment being terminated.

In Fig. 7, a graphical representation of the behaviour of the specimens during the tests is displayed. The characteristic points indicate the force at glass breakage ($P_{el,\max}$), the force drop ($P_{cr,\min}$), and the stable post-critical force ($P_{cr,\max}$) together with corresponding cross-head displacements: $u(P_{el,\max})$, $u(P_{cr,\min})$ and $u(P_{cr,\max})$, respectively.

Table 2 summarises all results obtained from experiments. A relatively small variation of the results was observed, which proves the correctness of the designed test stand and the correctness of the experimental methodology.

In Fig. 8a, the average $P_{el,\max}$ values at glass breakage are displayed, regardless of the reinforcement diameter. A clear pattern emerges, with the strength increasing as the glass thickness grows. However, when examining these values with respect to the reinforcement diameter, a surprising relationship is revealed. Fig. 8b compares the mean $P_{el,\max}$ forces, and standard deviations for reference and reinforced samples. It becomes apparent that the force decreases as the mesh reinforcement diameter increases. This phenomenon may be caused by local stiffening of the laminate, which may have led to premature fracturing of the glass observed in experiments. Glass as a material is very sensitive to point stress concentrations [23]. Larger diameters of steel mesh discs cause local stiffening of the panels around the point fixing. The greater rigidity of the glass panels causes that within the connection itself (metal fittings), there is a compensation of deformations and "local rotation". The decrease in the recorded forces' value will be caused by local deformations within the metal fitting itself and

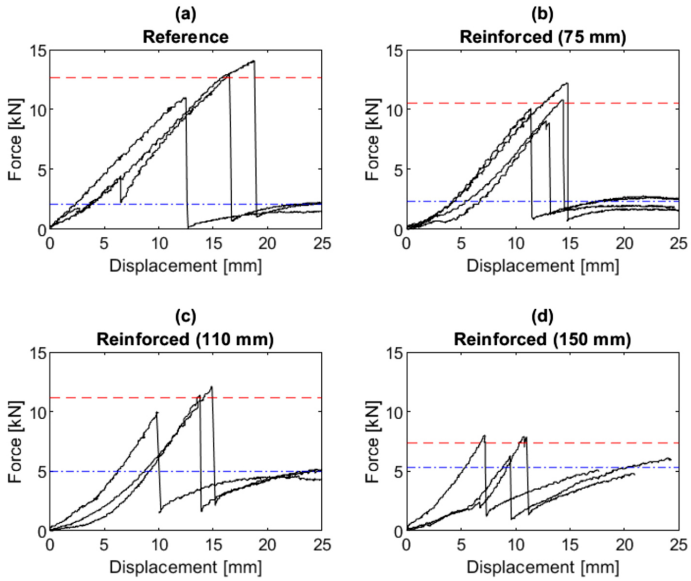


Fig. 6. Results of experiments for G10 series: force–displacement histories for reference and reinforced samples. Red lines indicate the average maximum force at glass fracture, while blue lines represent the average maximum force in the post-breakage phase

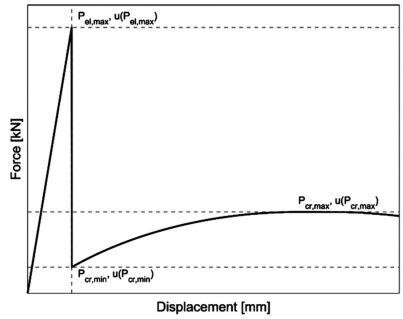


Fig. 7. Representation of the global behaviour of the specimens during the test

the pressure of the glass edge against the metal fitting. In this case, an important conclusion will be the appropriate treatment of these edges with glass. In the next stages of the research, additional rounding, machining and blunting of the edges of the glass panes will be justified. These technological measures should eliminate local stress concentrations on the edges of the glass in the point fastenings of the joints. This procedure will increase the guaranteed load capacity of these connections. It should be remembered that glass itself (as a material) in a pure compression test achieves very high levels of breaking stress. Local deformations and local stress concentrations determine the destruction of this material that we deal with when increasing the stiffness of the zone within the connection (larger mesh diameters).

Table 2. Results of the experimental study

| Test Series | $P_{el,\max}$ [kN] | $u(P_{el,\max})$ [mm] | $P_{cr,\min}$ [kN] | $u(P_{cr,\min})$ [mm] | $P_{cr,\max}$ [kN] | $u(P_{cr,\max})$ [mm] |
|---|---|---|---|---|---|---|
| G8-R | 7.43 ± 0.29 | 20.10 ± 2.36 | 0.40 ± 0.08 | 20.23 ± 2.38 | 1.60 ± 0.25 | 35.80 ± 3.90 |
| G8-75 | 7.90 ± 1.34 | 13.07 ± 3.36 | 0.83 ± 0.09 | 13.20 ± 3.36 | 2.07 ± 0.12 | 22.87 ± 2.87 |
| G8-110 | 6.80 ± 0.29 | 9.17 ± 0.74 | 1.57 ± 0.12 | 9.27 ± 0.74 | 3.23 ± 0.37 | 15.50 ± 1.81 |
| G8-150 | 5.63 ± 1.31 | 8.77 ± 0.81 | 1.27 ± 0.46 | 8.90 ± 0.79 | 4.50 ± 0.29 | 21.07 ± 3.35 |
| G10-R | 12.70 ± 1.28 | 15.83 ± 2.65 | 0.63 ± 0.33 | 16.13 ± 2.60 | 2.10 ± 0.36 | 27.03 ± 0.87 |
| G10-75 | 10.55 ± 1.13 | 16.73 ± 2.41 | 1.05 ± 0.32 | 16.98 ± 2.51 | 2.30 ± 0.46 | 23.53 ± 3.81 |
| G10-110 | 11.17 ± 0.87 | 12.80 ± 2.16 | 1.73 ± 0.26 | 13.07 ± 2.16 | 5.00 ± 0.29 | 23.57 ± 2.42 |
| G10-150 | 7.40 ± 0.78 | 9.10 ± 1.50 | 1.13 ± 0.17 | 9.40 ± 1.56 | 5.33 ± 0.56 | 20.63 ± 2.65 |
| G12-R | 16.55 ± 2.21 | 24.56 ± 5.05 | 0.74 ± 0.33 | 23.15 ± 4.59 | 2.8 ± 0.31 | 28.34 ± 3.01 |
| G12-75 | 19.13 ± 1.37 | 21.38 ± 2.96 | 2.68 ± 0.30 | 21.70 ± 3.07 | 4.23 ± 0.42 | 24.85 ± 2.74 |
| G12-110 | 13.47 ± 2.09 | 13.20 ± 1.77 | 2.53 ± 0.49 | 13.40 ± 1.82 | 6.67 ± 0.29 | 22.70 ± 2.12 |
| G12-150 | 16.10 ± 1.98 | 24.97 ± 8.06 | 3.37 ± 0.31 | 25.20 ± 8.05 | 7.67 ± 0.19 | 36.00 ± 7.81 |

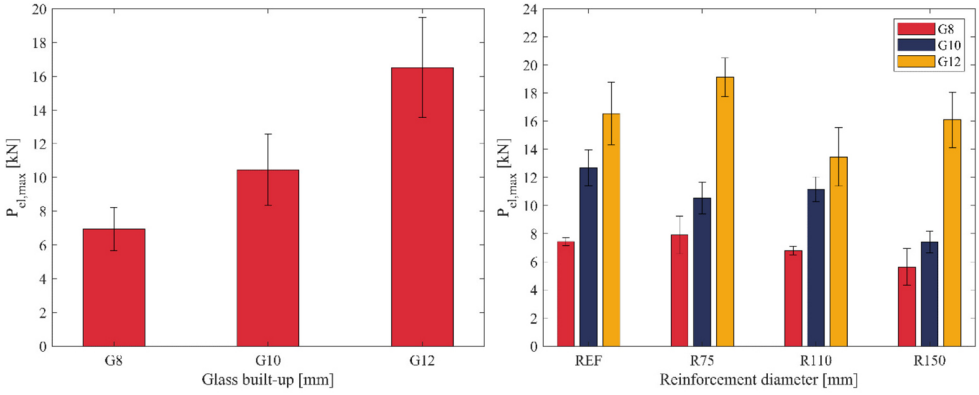


Fig. 8. Results of experiments: average $P_{el,\max}$ without considering the diameter of the reinforcement (a), variation of $P_{el,\max}$ depending on the thickness of the glass and the diameter of the reinforcement (b)

## 3.2. Failure modes

The addition of steel meshes as reinforcements in the tested glass samples significantly impacted the level of damage observed. As the thickness of the glass and the diameter of the steel spacers used in the samples increased, greater forces were recorded at the steel fittings (as shown in Table 2). These samples displayed “greater ductility”, and the damaged fittings remained stable even after glass breakage. Complete tearing of the sample required significant (four to five times greater) piston displacements in the testing machine to completely defragment the joint. These observations are crucial in ensuring the safety of using glass panels

with tested reinforcements. They also play an important role in determining the post-critical load capacity. Using steel meshes to reinforce the joints ensures a higher level of safety in the event of damage to the point-fixed element of the glass panel. Even after glass breakage, the connections with reinforcements hold the glass panes, ensuring the level of post-critical load capacity of the glass element indicated in the tests.

Fig. 9. View of damaged samples – reference sample (left), reinforced sample (right)

Upon examining the reference sample, it was observed that the construction pin (point connection) was torn, as depicted in Fig. 10. However, in the samples with mesh reinforcement, the fastener remained intact in the tested element even after sustaining damage from glass breakage. The thickness of these samples varied from 8 mm to 12 mm, as shown from left to right. Such reinforced samples displayed greater post-critical capacity, enhancing safety levels and reducing the chances of the panel detaching from the glass façade in real-world situations.

Fig. 10. View of damaged samples – reference sample (left), reinforced sample (right)

### 3.3. Post-breakage capacity

In the post-elastic phase, the post-breakage load capacity is determined by the increase in the stabilised force $P_{cr,\max}$. Fig. 11 compares the mean $P_{cr,\max}$ values for reference and reinforced samples. The force increases with the glass's thickness and the reinforcement's diameter. This tendency also applies to the thickness of the glass, as broken glass fragments assist in transferring loads in the post-critical phase. This may be caused by the force acting at an angle, the broken glass fragments wedge due to the pull-out force, or because there is a much larger compression zone.

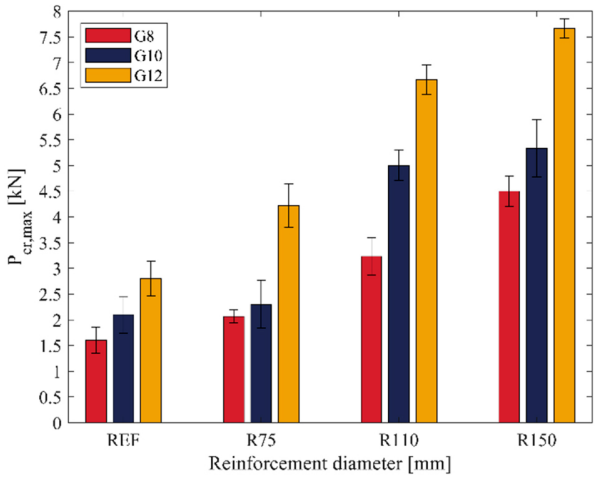


Fig. 11. Maximum force in the post-breakage phase $P_{cr,\max}$

The positive impact of the mesh embedded in the laminate is noticeable as the average force increases with the reinforcement diameter. Fig. 12 shows the percentage increase in $P_{el,\max}$ force of the reinforced samples compared to the reference specimens. According to the findings, incorporating mesh with 75, 110, and 150 mm diameters results in a 30%, 126%, and 170% increase in force $P_{el,\max}$, respectively.

## 4. Conclusions and further work

This article presents the results of experimental studies on the pull-through resistance and post-breakage capacity of laminated glass elements subjected to out-plane loading at an angle of 45°. The study involved reference (unreinforced) and reinforced samples with embedded steel woven mesh. This study has potential limitations. It is limited to three thicknesses of the component panes (8, 10 and 12 mm) and three diameters of the reinforcing inserts (75, 110 and 150 mm). Moreover, it should be noted that a displacement rate of 10 mm/min was applied in this study. Different rates could affect the results.

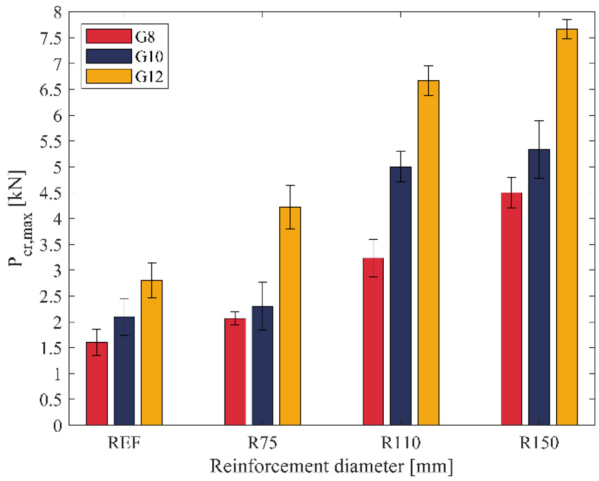


Fig. 12. Percentage increase in $P_{el,\max}$ force compared to the reference sample

The following conclusions can be drawn from the conducted research. It should be emphasized that the obtained results and conclusions pertain exclusively to the scope of the research conducted by the authors of this article.

- Samples reinforced with embedded steel woven mesh exhibit higher load transfer values than the reference samples.
- Failure of these reinforced elements is caused by local stress concentration points located directly in the fitting. The shape of the steel fittings, spacers, and the edge treatment of the glass in the hole for mounting the steel fittings greatly affect the damages incurred.
- The post-critical load capacity is increased with the use of mesh reinforcements. This makes them a reliable option for enhancing the safety of glass panels used in metal and glass facades. Even after damage, such as glass breakage, the panel remains secure in its original location and can be safely replaced.

## Acknowledgements

This research was funded by the National Centre for Research and Development (NCBR) within the research project “Innovative solution for point-fixed laminated glass with improved capacity after glass fracture” (Grant No. LIDER/34/0125/L-432 11/19/NCBR/2020, LIDER XI Program).

## References

[1] J. E. Shelby, *Introduction to glass science and technology*. Cambridge: Royal Society of Chemistry, 2020.

[2] A. Jóźwik, "Introduction to structural design of glass according to current European standards”, *Archives of Civil Engineering*, vol. 68, no. 2, pp. 147–170, 2022, doi: 10.24425/ace.2022.140634.

[3] X. Centelles, J. R. Castro, and L. F. Cabeza, "Experimental results of mechanical, adhesive, and laminated connections for laminated glass elements – a review", *Engineering Structures*, vol. 180, pp. 192–204, 2019, doi: 10.1016/j.engstruct.2018.11.029.

[4] M. Martín, X. Centelles, A. Solé, C. Barreneche, A. I. Fernández, and L. F. Cabeza, "Polymeric interlayer materials for laminated glass: A review", *Construction and Building Materials*, vol. 230, art. no. 116897, 2020, doi: 10.1016/j.conbuildmat.2019.116897.

[5] F. P. Bos, "Safety concepts in structural glass engineering: Towards an integrated approach", PhD thesis, Delft University, The Netherlands, 2009.

[6] A. Vedrtnam and S. J. Pawar, "Laminated Plate Theories and fracture of laminated glass plate – a review", *Engineering Fracture Mechanics*, vol. 186, pp. 316–330, 2017, doi: 10.1016/j.engfracmech.2017.10.020.

[7] K. Grębowski and A. Wróbel, "Architectural and Urban Planning Solutions for the protection of heritage buildings in the context of terrorist attacks: Following the example of Passive Protection Systems", *Buildings*, vol. 12, no. 7, art. no. 988, 2022, doi: 10.3390/buildings12070988.

[8] G. Royer-Carfagni and M. Silvestri, "Fail-safe point fixing of structural glass. New advances", *Engineering Structures*, vol. 31, no. 8, pp. 1661–1676, 2009, doi: 10.1016/j.engstruct.2009.02.050.

[9] C. Bedon, "Time-domain numerical analysis of single pedestrian random walks on laminated glass slabs in pre- or post-breakage regime", *Engineering Structures*, vol. 260, art. no. 114250, 2022, doi: 10.1016/j.engstruct.2022.114250.

[10] G. Castori and E. Speranzini, "Structural analysis of failure behavior of laminated glass", *Composites Part B: Engineering*, vol. 125, pp. 89–99, 2017, doi: 10.1016/j.compositesb.2017.05.062.

[11] M. Kozłowski, "Experimental and numerical assessment of structural behaviour of glass balustrade subjected to soft body impact", *Composite Structures*, vol. 229, art. no. 111380, 2019, doi: 10.1016/j.compstruct.2019.111380.

[12] C. Zhao, J. Yang, X. Wang, and I. Azim, "Experimental investigation into the post-breakage performance of pre-cracked laminated glass plates", *Construction and Building Materials*, vol. 224, pp. 996–1006, 2019, doi: 10.1016/j.conbuildmat.2019.07.286.

[13] X. Wang, J. Yang, W. T. Chong, P. Qiao, S. Peng, and X. Huang, "Post-fracture performance of laminated glass panels under consecutive hard body impacts", *Composite Structures*, vol. 254, art. no. 112777, 2020, doi: 10.1016/j.compstruct.2020.112777.

[14] I. Stelzer and M. Singh Rooprai, "Post Breakage Strength Testing for Overhead Laminated Glass", presented at Challenging Glass 5 – Conference on Architectural and Structural Applications of Glass, 16–17 June 2016, Ghent University, Belgium, doi: 10.7480/cgc.5.2265.

[15] A. H. C. Chen, and J. Yang, "Simulating the breakage of glass under hard body impact using the combined finite-discrete element method", *Computers & Structures*, vol. 177, pp. 56–68, 2016, doi: 10.1016/j.compstruc.2016.08.010.

[16] F. Bos, C. Louter, and F. Veer, "Structural Glass Beams with Embedded Glass Fibre Reinforcement," presented at Challenging Glass 2 – Conference on Architectural and Structural Applications of Glass, 20-21 May 2010, Delft University of Technology, The Netherlands, doi: 10.7480/cgc.2.

[17] C. Bedon and C. Louter "Structural glass beams with embedded GFRP, CFRP or steel reinforcement rods: Comparative experimental, analytical and numerical investigations", *Journal of Building Engineering*, vol. 22, pp. 227–241, 2019, doi: 10.1016/j.jobe.2018.12.008.

[18] M. Achintha and T. Zirbo "Developments in GFRP Reinforced Bolted Joints in Glass", presented at Challenging Glass 6 – Conference on Architectural and Structural Applications of Glass, 17–18 May 2018, Delft University of Technology, The Netherlands, doi: 10.7480/cgc.6.2153.

[19] M. Achintha and T. Zirbo "GFRP reinforced high performance glass–bolted joints: Concept and experimental characterization", *Construction and Building Materials*, vol. 274, art. no. 122058, 2021, doi: 10.1016/j.conbuildmat.2020.122058.

[20] M. Kozłowski, D. Wasik, and K. Zemła, „Monotonic and Creep Studies on the pull-through resistance of laminated glass with locally embedded steel mesh", *Materials*, vol. 15, no. 20, art. no. 7083, 2022, doi: 10.3390/ma15207083.

[21] EN 16612:2020 Glass in Building—Determination of the Lateral Load Resistance of Glass Panes by Calculation. CEN, 2020.

[22] EN 1993-1-1:2022 Eurocode 3: Design of Steel Structures—Part 1-1: General Rules and Rules for Buildings. CEN, 2020.

[23] M. Cwyl, R. Michalczyk, N. Grzegorzewska, and A. Garbacz, "Predicting Performance of Aluminum – Glass Composite Facade Systems Based on Mechanical Properties of the Connection", *Periodica Polytechnica Civil Engineering*, vol. 62, no. 1, pp. 259–266, 2018, doi: 10.3311/PPci.9988.

## Badania eksperymentalne połączeń punktowych metal-szkło z różnymi konfiguracjami zbrojenia siatką

**Słowa kluczowe:** szkło laminowane, połączenia punktowe, wzmocnienie, nośność pokrytyczna

### Streszczenie:

Artykuł dotyczy zjawiska nośności pokrytycznej elementów mocowanych punktowo wykonanych ze szkła laminowanego. Przedstawia wyniki projektu badawczego mającego na celu opracowanie wzmocnionego, mocowanego punktowo elementu wykonanego ze szkła laminowanego z lokalnie osadzoną siatką stalową. Łącznie przebadano 36 próbek (300 mm × 300 mm) różniących się grubością tafli (8, 10 i 12 mm) oraz średnicą siatki wzmacniającej (75, 110 i 150 mm). Próbki składały się z dwóch tafli szkła hartowanego, folii EVA Clear oraz plecionej, stalowej siatki wykonanej z drutów o średnicy 0,35 mm w rozstawie 1 mm × 1 mm. Badania prowadzono w przestrzennej maszynie wytrzymałościowej umożliwiającej obciążanie łącznika punktowego pod kątem 45 stopni. Ten sposób obciążenia łącznika odpowiada jego stanowi obciążenia w rzeczywistym zastosowaniu (np. szklany daszek z wieszakami). Wszystkie próbki wykazały podobne zachowanie w czasie badań. W pierwszej fazie zależność między obciążeniem a przemieszczeniem odnosi się do sprężystej odpowiedzi próbki na obciążenie. Po zarysowaniu szkła następuje nagły spadek siły z powodu utraty sztywności na rozciąganie zarysowanego szkła hartowanego. Po tym etapie następuje postępująca degradacja próbek w wyniku dalszego obciążania. W tej fazie siła początkowo rośnie, po czym ulega stabilizacji – ten punkt jest uważany za obciążenie graniczne (w stanie pokrytycznym) i eksperyment przerwano. W przypadku wszystkich serii badawczych, osadzenie siatki stalowej w warstwie folii zwiększyło nośność w stanie pokrytycznym. Badania przeprowadzono w ramach projektu badawczego Innowacyjne rozwiązania dla szkła laminowanego mocowanego punktowo o zwiększonej nośności pokrytycznej" finansowanego przez Narodowe Centrum Badań i Rozwoju w ramach Programu LIDER XI.

Received: 2023-11-07, Revised: 2023-12-28